Modification of Spacecraft Potentials by Thermal Electron Emission on ATS-5

Richard Christopher Olsen*

The University of Alabama in Huntsville, Huntsville, Ala.

Electron emission experiments on Applied Technology Satellite 5 using a thermal electron emitter are reported and analyzed. Operations in eclipse charging environments showed that electron emission could partially discharge a negatively charged satellite. Typical operations resulted in kilovolt potentials being reduced to hundreds of volts for a few tens of seconds, followed by a gradual recharging over a period of minutes. Equilibrium currents were modeled with a one-dimensional current balance model. Currents on the order of 1 μA were found, significantly below emitter capabilities. Application of a three-dimensional, time-dependent computer model showed that differential charging on the solar arrays was limiting the emitted current, preventing the complete discharge of the satellite, and allowing it to recharge in spite of the electron emitter.

Introduction

DATA from applied Technology Satellite-5 (ATS-5) showed the existence of large electrostatic potentials on satellites at geosynchronous altitude. These potentials were explained as the result of a balance between the ambient plasma currents and secondary fluxes emitted from the spacecraft surface.[1,2] In 1974, a program of operations was begun to study means of modifying spacecraft potentials. The filament neutralizers on the ion engine experiment were used to emit thermal electrons in attempts to discharge ATS-5 in eclipse periods.

The program had mixed results. The large potentials were usually reduced in size, but the spacecraft was rarely totally discharged in this manner.[3] Modeling of these operations was done with one-dimensional current balance models and a more sophisticated three-dimensional program. It was found that the neutralizer filament emission was limited by a potential barrier developed by differential charging on the spacecraft surface.

The following sections repeat some of DeForest's development of spacecraft charging measurements and one-dimensional current models[1,2] show data from three neutralizer operations, and then show results from applying one-dimensional and three-dimensional models to the neutralizer operations.

Satellite and Instrumentation

ATS-5 was launched into synchronous orbit on August 12, 1969. Its final orbit was at 105° W longitude, with a spin rate of about 100 rpm about a spin axis nominally parallel to the Earth's axis. The spacecraft, illustrated in Fig. 1, was cylindrical, with an exterior dominated by solar arrays. Cavities at the top and bottom contained a mixed assortment of insulators and conductors. The fiberglass bellyband was the location of the majority of the instruments and experiments. These provided the majority of the conducting area on the spacecraft.

The plasma detectors were electrostatic analyzers for electrons and ions from 50 eV to 50 keV in 62 exponential steps, and had 12% energy resolution. One energy scan requires approximately 20 s. One pair of detectors was aligned

to the spin axis (nominally parallel to the magnetic field), with the other pair perpendicular to the spin axis and the magnetic field.[1]

The ion engines were small cesium thrusters with filament neutralizers. The engines were only operated briefly, due to the spinup of the spacecraft, but the filaments were unaf-
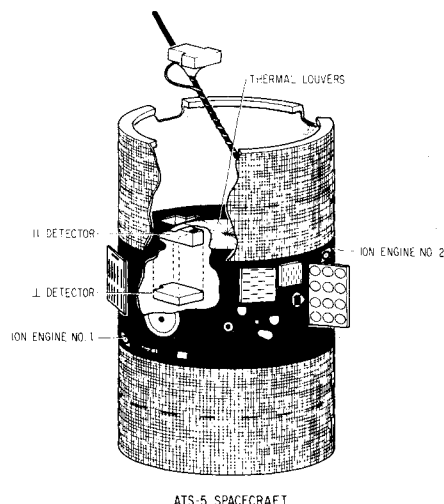

ATS-5 SPACECRAFT

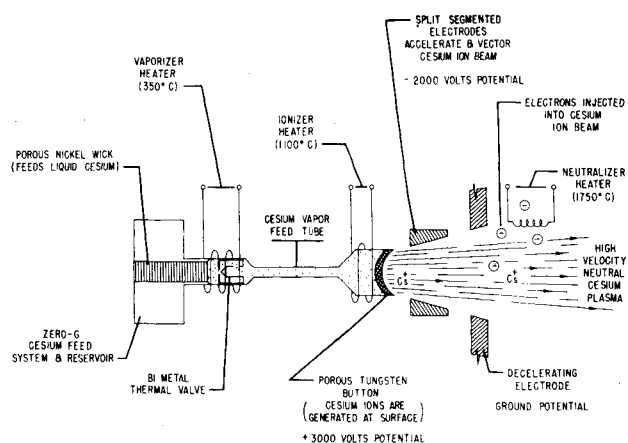**Fig. 1 ATS-5 spacecraft.**

Fig. 2 ATS-5 ion engine experiment.

*Research Associate, Physics Department. Member AIAA.

fected by the spinup. The filaments, illustrated in Fig. 2, can be seen near the outer edge of the thruster. A voltage drop of a few volts across the filament provided a small range of emitted energies in the electron-volt region.

Eclipse Charging

Data from a typical eclipse charging event are presented in Fig. 3. Figure 3 shows the particle fluxes found prior to and during the eclipse on October 16, 1969. The differential energy flux is roughly proportional to count rate, using a conversion factor of 4.3×10^{-5} cm^2-s, $(\Delta A \Delta \Omega \Delta E/E)$. Data taken from the perpendicular detector in sunlight are shown on the left-hand side of Fig. 3, with eclipse data on the right-hand side. In sunlight, the electron fluxes are one to two orders of magnitude higher than the ion fluxes, and the two distributions both peak smoothly near 10 keV. In eclipse, the

electron flux drops, as does the low-energy ion flux. A peak forms in the ion flux, and the fluxes above this energy are elevated. The eclipse data have been successfully interpreted as the result of a -4.2 kV potential on the spacecraft with respect to the distant plasma. There is an absence of ions below this energy, with all the ambient ions accelerated to 4.2 keV or higher energy. Eclipse potentials ranged from 0 to -10 kV, and the example in Fig. 3 is typical for this satellite.

In 1974, data from the ATS-6 satellite presented similar results. Stationed at 94° W longitude, the newer satellite encountered almost the same environment as ATS-5. Potential measurements made in eclipse on the two satellites were remarkably close when the environment was constant over that distance. Because of this, it was possible to use ATS-6 data during operations of the ATS-5 filaments as a control for comparison purposes.[3]

Operations of the Filament Emitter

Data from a neutralizer operation on September 20, 1974 are presented in Figs. 4 and 5. The ATS-5 data are presented in a 2-h spectrogram covering the eclipse period in Fig. 4, while Fig. 5 gives the potentials on both satellites during the operation. A spectrogram is a gray-scale presentation of the plasma data where low count rates are plotted as black or dark gray, and higher count rates as light gray or white. The energy scales both start at 0 eV in the center, increasing up and down to 50 keV, for electrons and ions, respectively. The time scale on the horizontal axis runs from 06:00 to 08:00 UT. The spectrogram shows an energetic but relatively constant environment in the midnight region. Strong electron fluxes are visible up to 20 keV. The large spacecraft potentials in eclipse are again shown by the absence of ions below the large charging peak. The ATS-6 potential varies between -1 and -4 kV, as does the ATS-5 potential when the neutralizer is off. The ATS-5 eclipse period ran from 06:23 to 07:30, and ATS-6 was eclipsed from 05:37 to 06:42. The ATS-5 spectrogram shows the abrupt rise in potential caused by the neutralizer operation from 06:31:25 to 06:35:25. A later
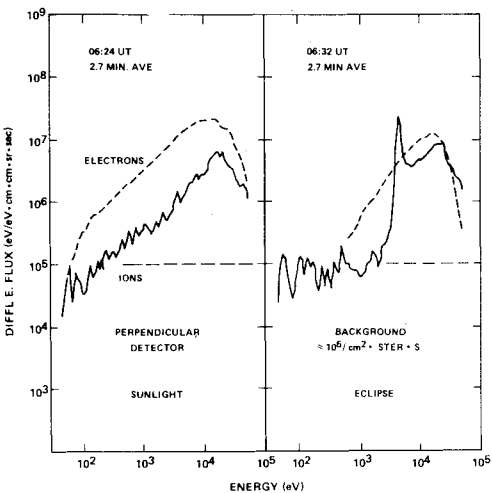

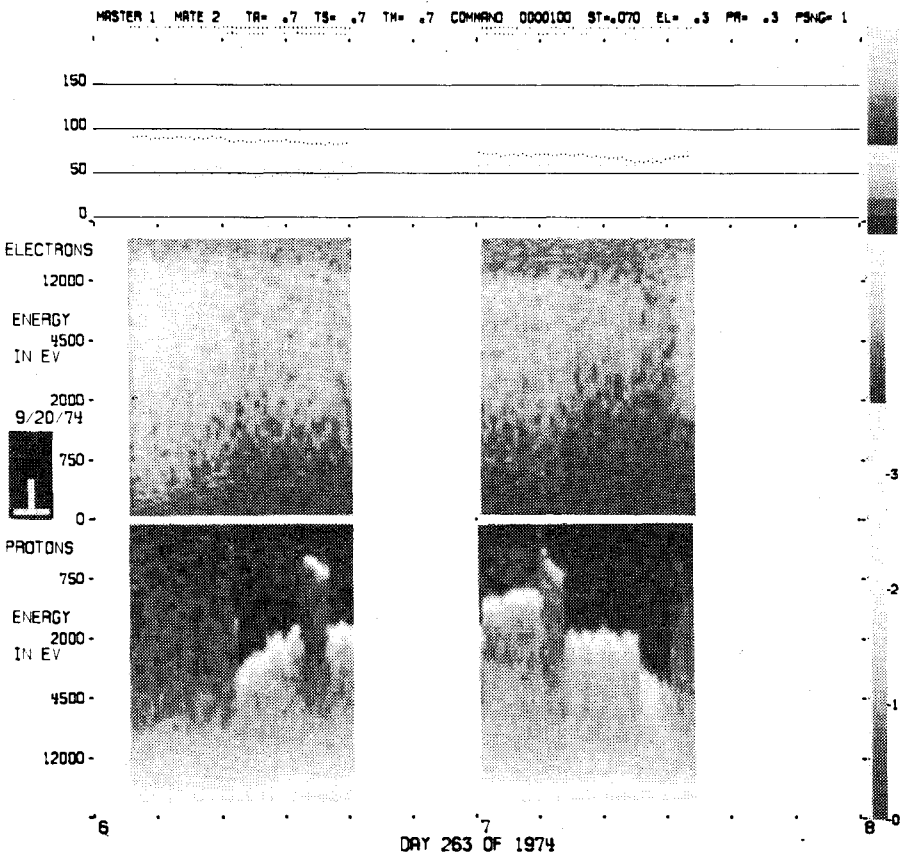Fig. 3   ATS-5 eclipse charging, October 16, 1969.

Fig. 4   ATS-5 spectrogram, September 20, 1974.

operation, from 07:05 to 07:09 also shows an abrupt rise in potential during the neutralizer operation, with variations in potential during the operation. Figure 5 presents a more detailed look at the first operation of the day. The potentials of the two spacecraft were determined by using the cutoff in the ion data due to the acceleration of low-energy ions up to the spacecraft potential. The values would be subject to about ±5% error due to the energy window width for an ideal detector. A missing data point, as is occasionally encountered on ATS-5, will result in a value which is about 10% to 20% too negative. ATS-5 responds immediately to the neutralizer "on" command, rising to near zero potential between two data points. There is a smooth drop in the potential following the initial discharge peak. The neutralizer "off" command is followed by an immediate drop in potential to the equilibrium eclipse value.

Similar behavior is seen in Fig. 6, where data from September 30, 1974 are presented. Again, the rapid discharge and then recharging of the satellite is apparent. The variation in the charging rate after the initial discharge spike is again seen. The neutralizer is operated from 06:34:20 to 06:38:20. Initially, from 6:35 to 6:36 the potential changes by 450 V. By 6:37, the rate of change is only 100 V/min. The question this raises is: Will the spacecraft potential reach an equilibrium in a longer operation?

As longer operations were run, it was found that the charging rate slowed to near zero after several minutes. However, another time-dependent effect became apparent. In some operations, there was a short but noticeable undershoot in the potential when the neutralizer was turned off; i.e., the potential became more negative than the normal equilibrium potential in eclipse would have been.

This effect can be seen in the data from March 28, 1978 in Fig. 7. The dip visible at 04:41 is one of the most pronounced such events. Typically, the dip would only last through one or two energy scans, i.e., 20-40 s. This dip in potential was at first thought to be an anomaly in the data, but repeated appearance of the phenomenon during such operations indicated it was a real effect.

Summary of Emitter Operations

Data from three of the 194 days of operations have been shown. The commonly seen features are the sharp rise in potential at the neutralizer "on" command, occasionally to above the −50 V limit of the particle data. This was followed by a rapid drop in spacecraft potential, a drop which slowed

as the potential seemed to approach a new equilibrium. It was found that whenever the spacecraft had charged negatively in eclipse, operation of the filament could partially discharge the spacecraft, but the neutralizer was most effective at low or moderate potentials. Figure 8 shows the results of a comparison of the spacecraft potential with the neutralizer off, and then the equilibrium value with the neutralizer on for 70 cases. Most spots indicate multiple measurements at a given pair of potentials. The diagonal line shows the neutralizer "on" equals neutralizer "off" locus. Potentials for neutralizer off were taken as an average around the operation time, and potentials for neutralizer on were taken after the neutralizer had been on for 1 or 2 min. The neutralizer consistently causes the spacecraft to discharge, with relatively greater effects at lower equilibrium eclipse potentials.

Charging Models

The objective of the analysis of these events was to determine the currents necessary to discharge the satellite. This required the development of a model for the equilibrium current balance to the spacecraft, in order to estimate the portions of the current balance that could not be directly measured. Once it became clear that there were time dependences in the data, a second goal was to understand the physical processes causing these variations. The first model to be developed is an extension of the one-dimensional current
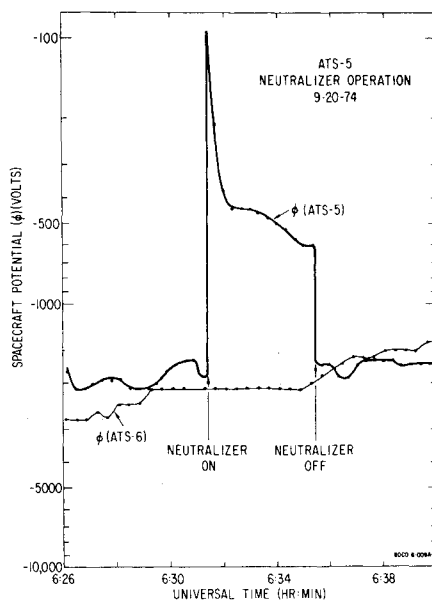

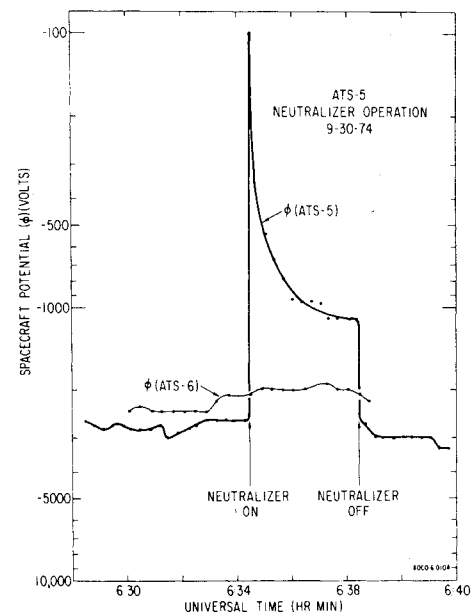Fig. 6 Neutralizer operation, September 30, 1974.

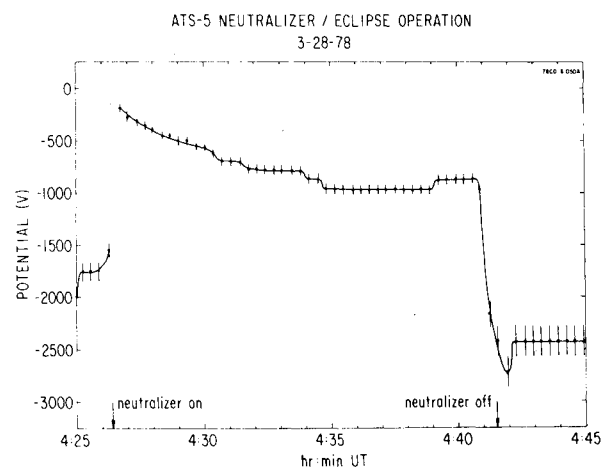Fig. 5 Neutralizer operation, September 20, 1974.

Fig. 7 Neutralizer operation, March 28, 1978.

balance model originally used to explain the ATS-5 charging behavior.[1] This model is an equilibrium model, and does not attempt to describe time-dependent changes. These latter effects were studied with NASCAP, a three-dimensional, time-dependent, charging analysis program.

One-Dimensional Current Balance Model

A one-dimensional current balance model was developed to model the equilibrium currents to the spacecraft. This was done in order to estimate the current emitted by the hot filament. The work followed the patterns established by earlier workers.[1-4] The plasma detectors measure the ambient fluxes which reach the spacecraft. These fluxes can then be used to calculate the secondary electron fluxes from the spacecraft.

Since the net current to the spacecraft should be zero in equilibrium, the use of an artificial source of particles will create an imbalance in the net flux to the spacecraft. There is an assumption here that the spacecraft has no current sinks, such as might be provided by differential charging.

The plasma detectors provided the 50-eV to 50-keV particle fluxes for the current measurement. In the environments studied, this energy range provides the bulk of the current to the spacecraft from the ambient plasma. It was assumed that the environment was isotropic, since the data quality and model could not support pitch angle anisotropy.
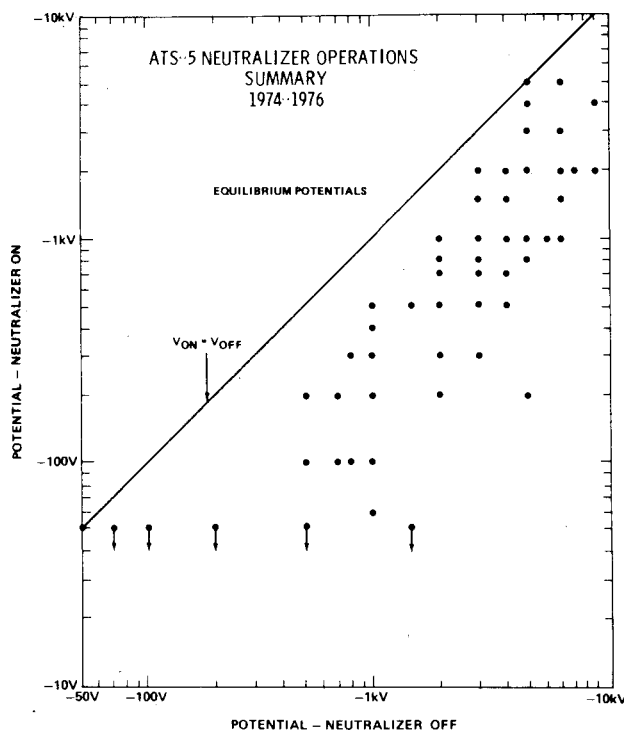
The primary problem with the data was the degradation of the electron sensors, i.e., the channeltrons. A recalibration of the detector was done by averaging the daily fluxes for selected days over the lifetime of the instrument (1969 to 1978), assuming that the flux was roughly constant at similar levels of magnetic activity, and renormalizing. The detectors were found to have dropped two orders of magnitude in sensitivity. The ion sensors were within a factor of 4 of their initial sensitivity. This recalibration introduces the possibility of a systematic error in the neutralizer current measurement of perhaps 50%.[5]

Secondary electron yields have been modeled as a function of the energy and angle of incidence for a great variety of materials. Since the spacecraft materials were not characterized before launch, material parameters for aluminum were used. These values would not be greatly different than those for the oxide coating on the solar arrays. The initial values for the true secondary yield for aluminum were a peak yield of 1 at 400 eV.[4-6]

The use of aluminum parameters for secondary yield required a calibration of the model to obtain more accurate numbers for the secondary yield. Data from 1969 and 1970 (prior to detector degradation) were used in the manner described by DeForest.[1] A slightly more extensive data set was used, with essentially the same results. The error measurement for the calibration was the net flux divided by the ambient electron flux. An rms error of 12% was found at the final calibration.

The current balance model was applied to the ATS-5 electron emitter operations, with results shown in Table 1. The net fluxes are now a measure of the current emitted by the hot filament. Conversion from flux to current requires integration of the flux over the area of the spacecraft. The question of which surface area to use becomes apparent at this time. The current balance the neutralizer is involved in is the balance to the mainframe of the spacecraft. The conducting area of the spacecraft is therefore the area to use in the integration. The cylindrical spacecraft has the dimensions: length $= 184$ cm, diameter $= 146$ cm, for an area of 12 m^2, neglecting the interior walls of the cavities. The conducting area is not accurately known, but is about one-tenth of the total area. The results of the ATS-5 modeling program are reported for nine cases in the form of current densities. The maximum current density is the value obtained at the maximum (least-negative) potential. The equilibrium value is obtained 1 or 2 min into the operation, after the rapid changes in potential have ceased. The equilibrium potential is the spacecraft potential before the emitter is used. Potentials are in kilovolts, current densities are in picoamps/cm^2.

Net fluxes of 30 pA/cm^2 were obtained from the equilibrium data, with maximum values of 60 pA/cm^2 obtained at the discharge peak. This gives an equilibrium current of 0.3 μA, assuming a conducting area of 1 m^2. The equilibrium current of 0.3 μA was substantially below the
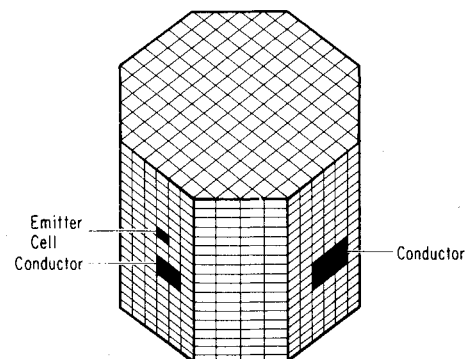

Fig. 8   Summary of ATS-5 neutralizer operations.

Table 1   ATS-5 neutralizer emission results

Date	Time	Equilibrium potential	Maximum current	Equilibrium current
9-19-74	07:15	−6.0	45.	10.
9-20-74	06:33	−2.0	60.	30.
9-30-74	06:36	−2.7	45.	30.
9-30-74	07:15	−1.9	60.	20.
10-1-74	06:35	−1.0	30.	20.
10-2-74	06:36	−7.0	35.	25.
10-4-74	06:40	−0.1	−15.	−10.[a]
10-7-74	06:45	−1.1	25.	10.
10-7-74	06:56	−0.6	15.	10.

[a] Spacecraft may have gone positive during emitter operation.

Fig. 9   NASCAP/ATS-5 model object.

Table 2   ATS-5 object material properties

Property	Aluminum	SiO_2
Dielectric constant	1	4
Thickness, m	1×10^{-3}	2.75×10^{-4}
Bulk conductivity, mho/m	...	2.75×10^{-12}
Atomic number	13	13
Maximum secondary yield	2.4	2.4
Energy, keV, for max. yield	0.35	0.35
Backscatter-range parameters[a]		
P7	260	260
P8	1.3	1.3
P9	240	240
P10	1.73	1.73
Yield for 1-keV ions	0.7	0.7
Ion energy, keV, for maximum yield	40	40
Photoelectron yield in sun, A/m^2	0^b	0^b
Surface resistivity	...	...

[a] Range (Å) = $P7E^{P8} + P9E^{P10}$, E in keV. [b] No photoemission except from emitter spot.
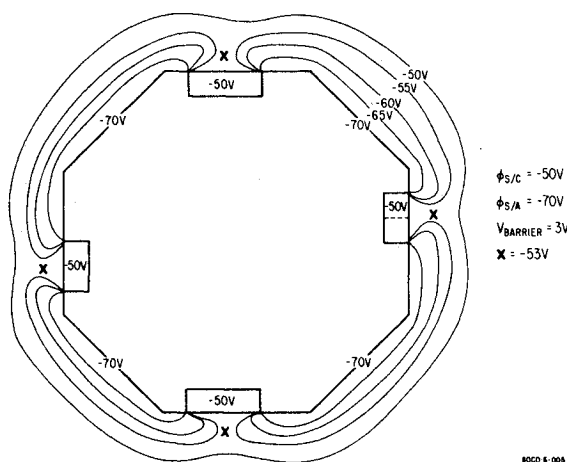
Fig. 10   ATS-5 object potential contours.

capabilities of the emitter (nominally milliamps). This fact, coupled with the peculiar time dependence of the potentials, lead to a consideration of how the current might be limited.

Space-charge effects were considered, but they could not explain the observed time dependences. Most reasonable space-charge-limiting processes would occur much more rapidly than the effects seen on ATS-5.

The solution was found to involve differential charging of the spacecraft surfaces. Because the majority of the spacecraft surface is insulating, it is able to hold a potential substantially different from the spacecraft mainframe. It will be shown below that such potentials can limit the neutralizer current. Finally, because of the difference in magnitudes of the spacecraft to plasma capacitance ($\sim 10^{-10}$ F) and solar array to mainframe capacitance ($\sim 10^{-6}$ F), the two time constants observed in the data are explainable as the time constants of the two capacitances. This will be seen in the time-dependent model below.

Three-Dimensional, Time-Dependent Modeling

The twin problems of a limiting process and time dependence require a code which can calculate fluxes to a three-dimensional object, and do so for the time-dependent case of switching on and off an artificial current. A three-dimensional analysis is required to obtain the electrostatic barrier generated by an uneven distribution of surface potentials.

The NASCAP (NASA Charging Analyzer Program) code was developed for the solution of equilibrium and time dynamic charging problems in magnetospheric environ-

ments.[6,7] Objects are modeled on a $16 \times 16 \times 33$ grid, with up to 15 different materials. The internal capacitances of the spacecraft are defined and calculated, as is the capacitance of the spacecraft to the distant plasma. Space-charge effects are left out, and Laplace's equation is used to determine the potentials in space around the object. Given an initial potential distribution on the spacecraft, the fluxes to the spacecraft are calculated based on a specified environment. A one-dimensional (spherical) approximation is used to calculate the flux to each surface. Secondary fluxes emitted from those surfaces are calculated based on the ambient fluxes. The effects of local electric fields on those emitted currents, i.e., barrier effects, are included, and can limit the emitted secondary electric flux. Barrier effects are also checked in the photoemission flux calculation. The code then works in cycles, calculating the change in potentials and fields caused by the current flow, then the new currents in the new electric field distribution. The accuracy of the code is largely a question of how accurately the material properties are known.

The ATS-5 satellite was modeled as shown in Fig. 9, filling most of the first grid. The object is embedded in a larger grid which is twice the size of the inner grid. In the ATS-5 object shown in Fig. 9, small conducting areas (dark) are surrounded by insulators (light).

The secondary emission properties of all surfaces are those of aluminum, a concession to a lack of knowledge of ATS-5 surface properties. The insulators and conductors differed only in their resistivity in the model object. Parameters are given in Table 2.

In the initial computer runs, potential distributions were established on the spacecraft in order to study the resulting fields. The objective was to establish an electrostatic barrier to electron emission. It was found that almost any nonuniform potential distribution did so! Figure 10 shows the results for a spacecraft at -50 V, with insulators at -70 V. The potential contours are given in the plane perpendicular to the spacecraft axis, midway along the axis. These conditions generated a saddle point at -53 V in front of the conducting surfaces, which results in a barrier of 3 V to electrons. Electrons emitted from the conducting spacecraft surfaces with less than 3 eV kinetic energy will be returned to the surface. This demonstrated that differential charging of the spacecraft could quickly lead to a limitation of the current emitted by the hot filament.

The final stage of the modeling was to attempt to duplicate the time dependence of the data. The electron emitter was modeled as a 10-μA source of photoelectrons, which the computer object emits with a thermal energy of 2 eV. Surfaces were given the secondary emission properties of aluminum. The model spacecraft had a capacitance to the distant plasma of 104 pF, and a much larger capacitance to the solar array of 1.3 μF. Thus the capacitance governing differential charging was 10,000 times larger than the capacitance corresponding to the mainframe to plasma potential difference. Given that the net current to the spacecraft at any time is roughly proportional to the potential of the spacecraft, an effective resistance can be invoked. When combined with the system capacitance, this gives an effective time constant for the time-dependent effects seen. The large difference in capacitances implies the time constants for charging and differential charging will show a substantial difference.

The results for a 10-keV Maxwellian environment are shown in Fig. 11. The solid line (with dots) shows the mainframe potential, with a scale to the left. The dashed line shows the differential potential, with a scale on the right axis. The noteworthy points here are not the magnitudes of the voltages, but rather the relative shape of the curves. At time zero the spacecraft is allowed to charge negatively to equilibrium. At 2 min, the emitter is started. The spacecraft discharged promptly (milliseconds). Until this time, no differential potentials had developed. The solar array now begins to charge negatively again, limited by the capacitance
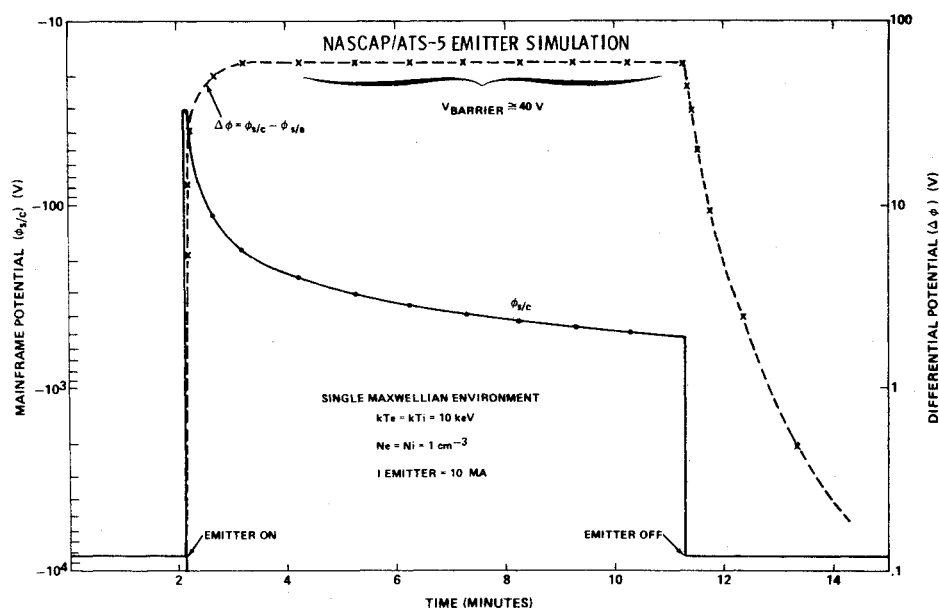
Fig. 11   ATS-5 NASCAP time sequence.

of the solar arrays to the spacecraft mainframe. Within 10 s, the solar array is 10 V negative with respect to the spacecraft, and a barrier is forming. Once a barrier has formed, the spacecraft potential drops back in the direction of its equilibrium eclipse value. The differential potential and barrier height stabilize, and the drop in potential slows. At emitter off, the potential promptly drops to the equilibrium value it had before the operation. This time development is identical to that seen in the actual operations. Different environments gave slightly different potentials, but the same time dependences and curve shapes were found.

The analysis shows that the differential charging initially develops on a time scale (seconds) faster than can be resolved with the plasma data. The gradual variations in potential seen in the data correspond to a time period when the differential potential, and resulting barrier, are nearly constant. The initial charging spike, and development of differential charging, are the result of the substantial positive current being emitted by the object. Once the barrier forms, the large positive current is greatly reduced, the object receives a much smaller net negative current, and the potential varies on a much slower time scale (10's of seconds), which is observed.

The negative overshoot at emitter off was seen in a few of the model runs, but was not always seen. It seemed to depend upon the environment. The overshoot can be understood as part of this model. At the time the neutralizer is switched off, there is a differential potential on the spacecraft which is generating a barrier to low-energy electrons. There is no fundamental difference between the filament electrons and those generated by true secondary emission. If the environment is such that the true secondaries are an important part of the current balance, a barrier around the conductors will seriously affect the current balance to the spacecraft even after the emitter is switched off. It can be seen in the figure that for this case, the differential potential has a time constant of about 1 min for decaying. This time constant depends on the interspacecraft capacitances, which are poorly determined. More accurate knowledge of the spacecraft structure, used in the right environment, should yield quantitative as well as qualitative agreement with actual operations.

Summary and Conclusions

The electron emitter on ATS-5 was operated over a hundred times over a 4-yr period. These operations succeeded in reducing the magnitude of the potentials on the satellite, but rarely discharged the spacecraft completely. Transient negative potentials of greater size than the eclipse equilibrium value were seen when the neutralizer was switched off.

Modeling of the current balance to the spacecraft showed that less than 1% of the emitted current was escaping the spacecraft at equilibrium. Three-dimensional modeling of the potentials and currents with NASCAP showed the development of differential potentials of on the order of 100 V to be developed on the spacecraft surfaces, limiting the emission of the filament. This limitation was sufficient to explain the equilibrium potentials seen, and would apply to most spacecraft with insulating surfaces. The NASCAP computer code was shown to be an effective tool in the modeling of three-dimensional charging problems, providing both the model of the limitation mechanism, and the model for the time development of the observed effects.

References

[1] DeForest, S.E., "Spacecraft Charging at Synchronous Orbit," *Journal of Geophysical Research,* Vol. 77, 1972, p. 651.

[2] DeForest, S.E., "Electrostatic Potentials Developed by ATS-5," *Photon and Particle Interactions with Surfaces in Space,* edited by R.J.L. Grard, D. Reidel, Holland, 1973, pp. 263-276.

[3] Goldstein, R. and DeForest, S.E., "Active Control of Spacecraft Potentials at Geosynchronous Orbit," *Spacecraft Charging by Magnetospheric Plasmas,* Progress in Astronautics and Aeronautics, Vol. 47, edited by A. Rosen, AIAA, New York, 1976, pp. 169-181.

[4] Whipple, E.C. Jr., "The Equilibrium Potential of a Body in the Upper Atmosphere and in Interplanetary Space," NASA Technical Note X-615-65-296, 1965.

[5] Olsen, R.C., *Differential and Active Charging Results from the ATS Spacecraft,* Ph.D. Thesis, University of California at San Diego, 1980.

[6] Mandell, M.J., Katz, I., Schnuelle, G.W., Steen, P.G., and Roche, J.C., "The Decrease in Effective Photocurrents due to Saddle Points in Electrostatic Potentials near Differentially Charged Spacecraft," *IEEE Transactions on Nuclear Science,* Vol. 6, (NS25), 1978, p. 1313.

[7] Katz, I. et al., *A Three Dimensional Dynamic Study of Electrostatic Charging in Materials,* NASA Contract Report No. 135256, Systems, Science, & Software Report 77-3367, 1977.